Multiple-Bridged Bis-Tetrathiafulvalenes: New Synthetic Protocols and Spectroelectrochemical Investigations

Holger Spanggaard,[†] Jesper Prehn,[†] Mogens Brøndsted Nielsen,*[,‡] Eric Levillain,*[,§] Magali Allain,[§] and Jan Becher*[,†]

Contribution from the Department of Chemistry, University of Southern Denmark (Odense University), Campusvej 55, DK-5230 Odense M, Denmark, Laboratorium für Organische Chemie, Eidgenössische Technische Hochschule (ETH), Universitätsstrasse 16, CH-8092 Zürich, Switzerland, and Ingénierie Moléculaire et Matériaux Organiques, CNRS UMR 6501, Université d'Angers, 2 Bd Lavoisier, F-49045 Angers, France

Received February 14, 2000

Abstract: Synthetic strategies for preparing dimeric tetrathiafulvalenes (TTFs) linked by either one, two, or four bridges have been developed. In particular, we report efficient few-step protocols for the preparation of face-to-face overlapped quadruple-bridged bis-TTFs. The ready interconversion of *cis* and *trans* TTFs in the presence of catalytic amounts of acid was implemented in one synthetic protocol as a way to control the isomeric outcome. The compounds were characterized by NMR spectroscopy, mass spectrometry, and elemental analysis. Moreover, the X-ray crystal structure of the macrocycle **4b** is presented and compared to semiempirical (PM3) geometry optimizations. Cyclic voltammetry and spectroelectrochemistry were used to describe the interactions established between two TTF units upon oxidation, that is, their ability to form mixed-valence complexes and π-dimers either intra- or intermolecularly. The length, flexibility, and number of bridging units in a bis-TTF, as well as the specific TTF positions being connected, determine the extent of these interactions. Thus, rigid linkers enhance the formation of intermolecular mixed-valence complexes. For **4b**, the absorption spectrum of this mixed-valence state of TTF in solution has been recorded for the first time. Finally, preliminary complexation experiments with different electron-deficient molecules are described.

Introduction

Tetrathiafulvalene (TTF) is a reversible and stable two-electron donor which has been intensively studied for more than two decades, mainly with the aim of developing low-temperature organic superconductors.[1] The appearance of metallic conductivity in cation radical salts of TTF requires intrastack mixed-valence (MV) interactions, whereas an integer valence generally results in insulating materials.[1,2] In solution, one-electron oxidation of TTF leads to the formation of both MV dimers and π-dimers. The mixed-valence state ($TTF_2^{\bullet+}$) occurs when the radical cation shares the positive charge with another not yet oxidized TTF. π-Dimers (TTF_2^{2+}) form when two radical cations associate in a complex. These aggregate species represent the solution counterpart of the two solid-state situations (conductor/insulator) and can be viewed as models able to anticipate the final stoichiometry of the material.[3] The MV and π-dimer equilibria are characterized by the following equilibrium constants:

$$K_{MV} = \frac{[TTF_2^{\bullet+}]}{[TTF][TTF^{\bullet+}]} \quad (1)$$

$$K_{\pi-dim} = \frac{[TTF_2^{2+}]}{[TTF^{\bullet+}]^2} \quad (2)$$

The kinetic constants of these equilibria are very fast.[4] Subtracting the Nernst equations for the oxidation potentials, E_1 (TTF/$TTF^{\bullet+}$) and E_1' ($TTF_2^{\bullet+}/TTF_2^{2+}$), affords the following relation:

$$E_1' - E_1 = \frac{RT}{F} \ln \frac{K_{MV}}{K_{\pi-dim}} \quad (3)$$

From eq 3 it follows that when $K_{MV} = K_{\pi-dim}$, the potentials E_1 and E_1' become identical. However, $K_{MV} > K_{\pi-dim}$ implies $E_1' > E_1$, and two waves are expected in the voltammogram, one for the oxidation of TTF and one for the oxidation of the MV complex. $K_{MV} < K_{\pi-dim}$ implies $E_1' < E_1$, and only one wave at the position of E_1 will be observed.

Spectroelectrochemistry provides a powerful tool for analyzing the π-dimer and MV formations. Indeed, the π-dimer generated upon electrochemical oxidation usually shows an intermolecular charge-transfer transition at a wavelength different from the intramolecular transition of the radical cation unit. Thus, $TTF^{\bullet+}$ absorbs at wavelengths of maxima 430 and

* To whom correspondence should be addressed. Fax: (+45 66158780). E-mail: jde@chem.sdu.dk.
† University of Southern Denmark.
‡ Eidgenössische Technische Hochschule.
§ Université d'Angers.

(1) (a) Williams, J. M.; Ferraro, J. R.; Thorn, R. J.; Carlson, K. D.; Geiser, U.; Wang, H. H.; Kini, A. M.; Whangbo, M. H. *Organic Superconductors* (*Including Fullerenes*); Prentice Hall: Englewoods Cliffs, NJ, 1992. (b) Bryce, M. R. *Chem. Soc. Rev.* **1991**, *20*, 355. (c) Schukat, G.; Fanghänel, E. *Sulfur Rep.* **1996**, *18*, 1.

(2) Torrance, J. B. *Acc. Chem. Res.* **1979**, *12*, 79.

(3) Torrance, J. B.; Scott, B. A.; Welber, B.; Kaufman, F. B.; Seiden, P. E. *Phys. Rev. B* **1979**, *19*, 730.

(4) Huchet, L.; Akoudad, S.; Levillain, E.; Roncali, J.; Emge, A.; Bäuerle, P. *J. Phys. Chem. B* **1998**, *102*, 7776.

10.1021/ja000537c CCC: $19.00
Published on Web 09/13/2000

Scheme 1. Possible Oxidation Route of a Bis-TTF (model 1)

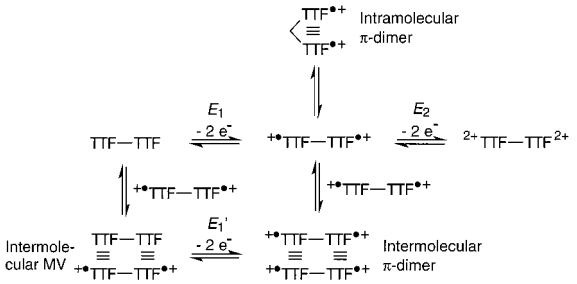

Scheme 2. Possible Oxidation Route of a Bis-TTF (model 2)

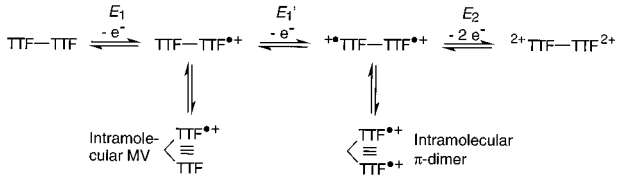

580 nm, whereas TTF_2^{2+} absorbs around 800 nm in acetonitrile.[4,5] For the dication TTF^{2+}, an absorption is observed at $\lambda_{max} = 390$ nm. In contrast, the absorption band of the mixed-valence state has never been identified in solution. However, it has been identified in polymeric films around 1800 nm, that is, as a low-energy transition.[4]

To elucidate the effect on the dimerization when two identical TTFs are covalently forced to be in close proximity, we decided to investigate a series of dimeric TTFs linked by more or less flexible linkers.[6] When oxidizing bis-TTFs, two models (Schemes 1 and 2) can be considered, depending on whether the TTFs are mono-oxidized in one or in two subsequent steps. In model 1 (Scheme 1), both TTFs are oxidized at the same potential, E_1. The resulting diradical cation may form intermolecular MV complexes as well as intermolecular π-dimers. In addition, intramolecular π-dimers may be formed if allowed to do so by the linkers. This model is basically the same as the above model for oxidation of TTF, with the only difference being that each process is a two-electron process because of the two units of TTF present. In model 2 (Scheme 2), originally proposed by Jørgensen et al.[7] for the oxidation of mono-bridged bis-TTFs containing $S(CH_2)_nS$ ($n = 1$, 2) linkers,[8] the two TTFs are oxidized sequentially at potentials E_1 and E_1' as two one-electron processes, forming an intermediate intramolecular MV complex.

Because of the four attachment sites, two TTFs can be covalently linked by one, two, three, or four bridges. In this work we have used both old and new synthetic protocols for obtaining a series of bis-TTFs, which differ in the number, size, and flexibility of their bridging units.

Results and Discussion

Synthesis. The preparation of 2,3-cyclized TTF macrocycles[9] were performed according to the stepwise strategy presented in Scheme 3. First, a dibromide (**2a**, **b**, or **c**) was reacted with the monothiolate of **1** produced in situ upon treatment with one equiv of CsOH,[10] affording the monobridged compounds **3a**−**c**.[11] Deprotection and alkylation with another equiv of **2a** or **b** under high-dilution conditions employing a two-syringe perfusor pump yielded the macrocycles **4a**,**b**[12] in high yields. The *tert*-butyl substituents on the phenyl group of the linkers impart solubility of the compounds in organic solvents. It was also possible to prepare the macrocycle **4a** in two successive deprotection/realkylation steps without intermediate workup. The macrocycle **4c**, containing phenolic bridging units, was prepared from alkylation of the bisthiolate of **1**. The two phenolic groups offer the possibility for incorporating **4c** into larger systems by *O*-alkylations. Unsymmetrical macrocycles (**5** and **6**) were prepared by reacting the monobridged bis-TTF **3b** with either bis(2-iodoethyl)ether or 1,2-bis(2-iodoethoxy)ethane.

(5) Some more or less contradictory results exist in the literature with respect to the π-dimer formation. The first electronic absorption spectrum of the TTF radical cation was reported in water, but no concentration or π-dimer formation data were mentioned: Wudl, F.; Smith, G. M.; Hufnagel, E. J. *J. Chem. Soc., Chem. Commun.* **1970**, 1453. Hünig et al observed no π-dimers of the TTF radical cation upon cooling an acetonitrile solution until crystallization occurred, whereas dimer formation was obtained for a dimethyldibenzo TTF derivative upon increasing the concentration or decreasing the temperature: Hünig, S.; Kiesslich, G.; Quast, H.; Scheutzow, D. *Liebigs Ann. Chem.* **1973**, 310. However, Torrance et al[3] identified dimers of the TTF radical cation in ethanol at 225 K. Furthermore, Huchet et al[4] observed a small but evident absorption peak resulting from dimers in acetonitrile (and in CH_2Cl_2/CH_3CN) at room temperature when oxidizing a relatively concentrated solution of TTF (ca. 5 mM). This absorption disappeared at low concentration (ca. 0.5 mM) but increased on a thin film of TTF-derivatized polythiophenes, confirming its assignment to a dimer.

(6) Review on bis-TTFs: Otsubo, T.; Aso, Y.; Takimiya, K. *Adv. Mater.* **1996**, *8*, 203.

(7) Jørgensen, M.; Lerstrup, K. A.; Bechgaard, K. *J. Org. Chem.* **1991**, *56*, 5684.

(8) The ability of very short bridges to facilitate the formation of an intramolecular MV complex has also been observed in the crystal structure of the radical cation salt of a TTF twin donor containing one methylenedithio bridging unit: Izuoka, A.; Kumai, R.; Sugawara, T. *Chem. Lett.* **1992**, 285. Oxidation of mono-bridged bis-TTF derivatives has also been studied by Cava and co-workers: Sudmale, I. V.; Tormos, G. V.; Khodorkovsky, V. Y.; Edzina, A. S.; Neilands, O. J.; Cava, M. P. *J. Org. Chem.* **1993**, *58*, 1355.

(9) Review on TTF macrocycles: Nielsen, M. B.; Becher, J. *Liebigs Ann.* **1997**, 2177.

(10) (a) Becher, J.; Lau, J.; Leriche, P.; Mørk, P.; Svenstrup, N. *J. Chem. Soc., Chem. Commun.* **1994**, 2715. (b) Lau, J.; Simonsen, O.; Becher, J. *Synthesis* **1995**, 521. (c) Simonsen, K. B.; Svenstrup, N.; Lau, J.; Simonsen, O.; Mørk, P.; Kristensen, G. J.; Becher, J. *Synthesis* **1996**, *3*, 407. (d) Becher, J.; Li, Z.-T.; Blanchard, P.; Svenstrup, N.; Lau, J.; Nielsen, M. B.; Leriche, P. *Pure Appl. Chem.* **1997**, *69*, 465.

(11) Compound **3a**: To a solution of **1** (1.03 g, 2.21 mmol) in dry DMF (50 mL) was slowly added (30 min) a solution of $CsOH·H_2O$ (0.390 g, 2.32 mmol) in dry MeOH (7 mL) under N_2, whereupon the mixture was stirred for 1 h. Then **2a** (0.49 g, 1.1 mmol) in dry DMF (6 mL) was added. The orange mixture was stirred for 30 min, after which the solvent was removed in vacuo. Column chromatography [silica, CH_2Cl_2] afforded an orange solid. Recrystallization from $CHCl_3$/MeOH gave **3a** as an orange glass (1.01 g, 82%): mp 62−63 °C; ^{1}H NMR ($CDCl_3$) $\delta = 7.20$ (s, 1H, ArH), 6.43 (s, 1H, ArH), 4.20 (t, 4H, $J = 6.5$ Hz, OCH_2), 3.16 (t, 4H, $J = 6.5$ Hz, SCH_2), 3.02 (t, 4H, $J = 7.2$ Hz, CH_2CN), 2.65 (t, 4H, $J = 7.2$ Hz, SCH_2) 2.43 (s, 12H, SCH_3), 1.36 (s, 18H, $C(CH_3)_3$); ^{13}C NMR ($CDCl_3$) $\delta = 155.57$, 131.82, 129.68, 125.36, 117.60, 109.00, 98.48, 66.82, 35.42, 34.42, 30.08, 19.11, 19.10, 18.59; MS(PD) $m/z = 1102$ (M^+). Anal. Calcd for $C_{40}H_{48}S_{16}O_2N_2$ (1101.79): C, 43.61; H, 4.39; N, 2.54; S, 46.56. Found: C, 43.64; H, 4.36; N, 2.49; S, 46.71.

(12) Compound **4a**: Method i: To a solution of **3a** (0.810 g, 0.74 mmol) in dry DMF (45 mL) was slowly added over 30 min a solution of $CsOH·H_2O$ (0.270 g, 1.62 mmol) in dry MeOH (5 mL) under N_2. Then the solution was stirred for 1 h. This mixture and a solution of **2a** (0.327 g, 0.75 mmol) in dry DMF (50 mL) were simultaneously added to dry DMF (50 mL) over 20 h by means of a two-syringe perfusor pump. The product was precipitated using H_2O (100 mL), filtered, and washed with MeOH (3 × 20 mL). Recrystallization from toluene/MeOH afforded **4a** (0.742 g, 79%) as an orange powder: mp 228−229.5 °C; ^{1}H NMR ($CDCl_3$) $\delta = 7.16$ (s, 2H, ArH), 6.32 (s, 2H, ArH), 4.09 (t, 8H, $J = 6.6$ Hz, OCH_2), 3.16 (t, 8H, $J = 6.6$ Hz, SCH_2), 2.44 (s, 12H, SCH_3), 1.33 (s, 36H, $C(CH_3)_3$); ^{13}C NMR ($CDCl_3$) $\delta = 155.21$, 129.49, 128.57, 127.67, 125.49, 111.61, 109.94, 97.39, 66.21, 34.85, 34.39, 30.09, 19.19; MS(PD) $m/z = 1270$ (M^+). Anal. Calcd for $C_{52}H_{68}S_{16}O_4$ (1270.32): C, 49.16; H, 5.41; S, 40.38. Found: C, 49.36; H, 5.43; S, 40.11. Method ii: To a solution of **1** (1.03 g, 2.21 mmol) in dry DMF (50 mL) was slowly added over 30 min a solution of $CsOH·H_2O$ (0.390 g, 2.32 mmol) in dry MeOH (7 mL), under N_2. Then the solution was stirred for 1 h, after which **2a** (0.49 g, 1.1 mmol) in dry DMF (6 mL) was added. The solution was stirred for 30 min, and then another solution of $CsOH·H_2O$ (0.390 g, 2.32 mmol) in dry MeOH (5 mL) was added over 30 min. After stirring for 1 h, this mixture and a solution of **2a** (0.490 g, 1.12 mmol) in dry DMF (50 mL) were simultaneously added together over 2 h. Then the solvent was removed in vacuo and the residue subjected to column chromatography [silica, CH_2Cl_2/cyclohexane 1:3], yielding **4a** (1.01 g, 72%) as an orange glass.

Scheme 3. Synthesis of Mono- and Dibridged Bis-TTFs

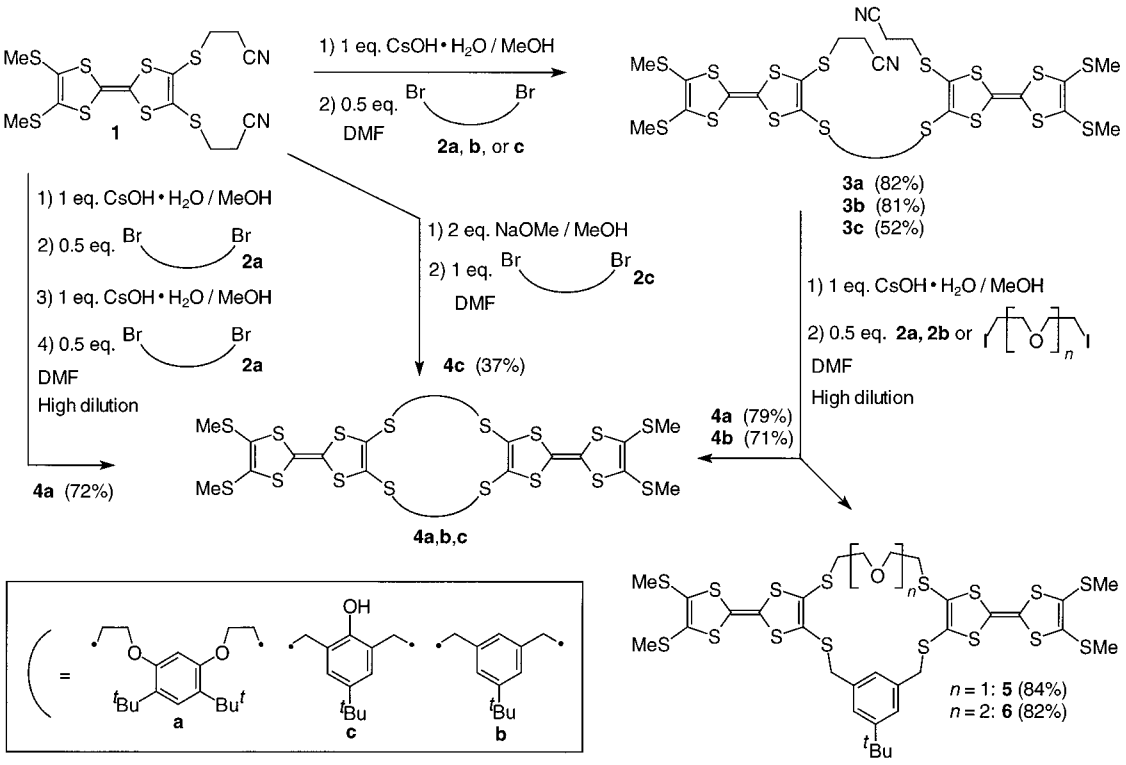

Scheme 4. Synthesis of a Macrocycle Containing Protected Thiolate Functions

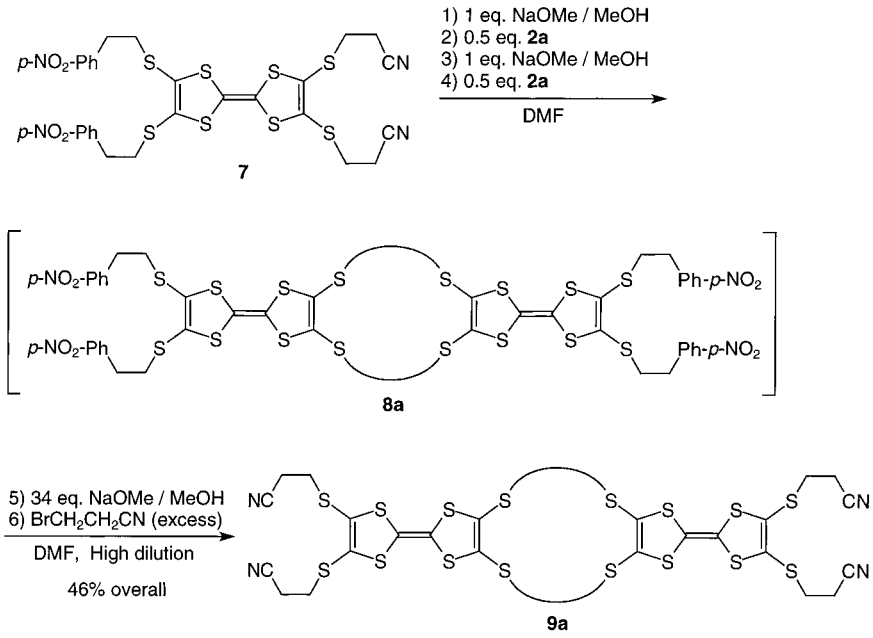

To prepare macrocyclic bis-TTFs containing cyanoethyl-protected thiolate groups in the 2,3-positions, we started out with the differentially protected 2,3-bis(2-cyanoethylthio)-6,7-bis[2-(4-nitrophenyl)ethylthio]tetrathiafulvalene **7** developed by Simonsen et al.[13] (Scheme 4). Adding 1 equiv of NaOMe removes one cyanoethyl group. Two of the resulting monothiolates were then linked together by alkylation with the dibromide **2a**. Deprotection and alkylation once more afforded the macrocycle **8a**, which was not isolated, but was converted into the macrocycle **9a**[14] by an interchange of protecting groups. We found that, although 1 equiv of base led to a quantitative removal of cyanoethyl, more equivalents were necessary to remove 4-nitrophenylethyl, and the elimination product, *p*-nitrostyrene, is usually difficult to remove in the purification process. For these reasons, we decided to isolate a cyanoethyl-protected macrocycle.

Macrocycle **9a** may find wide applications in synthetic TTF chemistry because of the possibility of its reacting further at the four protected thiolate groups. Thus, it can be used as a precursor for the preparation of quadruple-bridged bis-TTFs. Removal of all four cyanoethyl groups by adding 4.5 equiv of NaOMe, followed by the addition of 2 equiv of the dibromide **2a**, resulted in formation of the belt-type[15] compound **10a**[16] in an excellent yield of 68% (Scheme 5, route i). This same

(13) Simonsen, K. B.; Svenstrup, N.; Lau, J.; Thorup, N.; Becher, J. *Angew. Chem., Int. Ed. Engl.* **1999**, *38*, 1417.

Scheme 5. Synthesis of a Face-to-Face Overlapped Quadruple Bridged Bis-TTF (TTF-Belt)

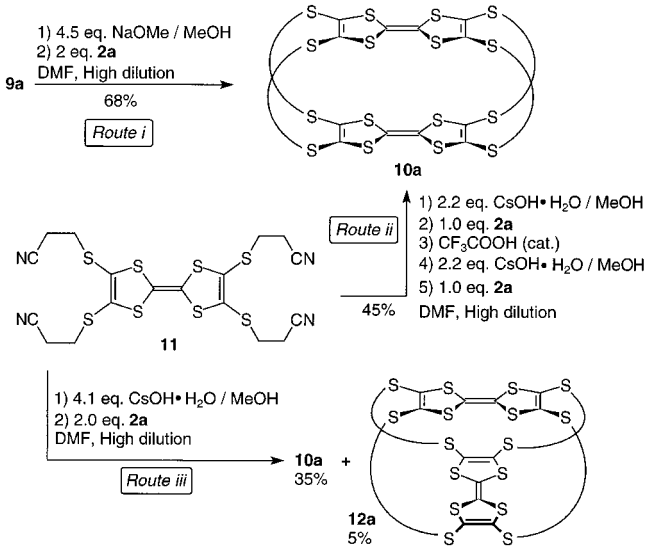

compound was synthesized earlier by less efficient and time-consuming stepwise mono-deprotectection/mono-realkylation steps.[13]

We previously reported about the construction of bicyclic systems that employ the selective 2,7(6)-deprotection of tetrakis-(2-cyanoethylthio)tetrathiafulvalene (**11**).[17] This time, we investigated whether **10a** could actually be prepared from sequential deprotection/alkylation steps of **11** without intermediate purifications (Scheme 5, route ii). Thus, **11** was first treated with 2 equiv of base and then 1 equiv of **2a**, which yielded the macrocyclic intermediate **13a** (Scheme 6) as a mixture of *cis*/*trans* isomers. It was evidenced from ^{1}H NMR measurements that adding catalytic amounts of trifluoroacetic acid to this isomeric mixture caused isomerization[18] to one stable isomer. This stable isomer seems to be the *cis*,*cis* isomer, because subsequent deprotection and alkylation steps (Scheme 5, steps 4 and 5, route ii) yielded the TTF-*belt* **10a**[16] in a yield of 45%. If present, a *trans*,*trans* precursor should result in a mixture of face-to-face and criss-cross overlapped macrocycles. Thus, by performing a simple acid-induced isomerization reaction before the final ring-closure, we are able to control the isomeric purity.

When all four thiolate functions were deprotected at once and bridged together upon reaction with **2a**, we obtained **10a**

Scheme 6. Intermediate in the Stepwise Synthesis of TTF-Belt **10a**

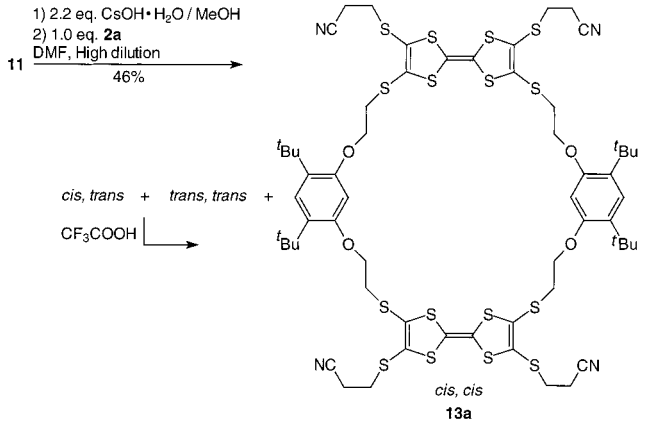

in a yield of 35% and the criss-cross overlapped macrocycle **12a** as a byproduct (5%) (Scheme 5, route iii). In this one-pot reaction,[16] the formation of **12a** is explained by the presence of *trans*,*trans* intermediates that contain two or three bridging units. Still, **10a** is the predominant product. It is compelling that a step involving eight bond-forming reactions among six separate species results in a belt molecule in such a remarkably high yield and that competing oligo- and polymerizations account for a maximum of 60% of the byproducts. Thus, it seems that the reactants, to a high degree, are preorganized for the belt-forming reaction.

(14) Compound **9a**: To a solution of **7** (0.259 g, 0.351 mmol) in dry DMF (30 mL) was added 0.5 M NaOMe/MeOH (0.75 mL, 38 mmol) over 20 min, under N_2. The solution was stirred for 20 min, after which **2a** (0.0766 g, 0.176 mmol) in dry DMF (40 mL) was added. The mixture was stirred for 10 min, after which 0.5 M NaOMe (0.75 mL, 0.38 mmol) was added. After stirring for 10 min, this mixture and a solution of **2a** (0.0763 g, 0.175 mmol) in dry DMF (40 mL) were simultaneously added over 1 h to dry DMF (30 mL). The mixture was stirred for 10 min, after which 0.5 M NaOMe/MeOH (24 mL, 12 mmol) was added. After stirring for 10 min, 3-bromopropionitrile (6 mL, 74 mmol) in DMF (20 mL) was added. After stirring for another 10 min, the solvent was removed in vacuo and the residue subjected to column chromatography [silica, (i) CH_2Cl_2/petroleum ether 3:1, (ii) CH_2Cl_2]. Recrystallization from $CHCl_3$/MeOH yielded **9a** (0.114 g, 46%) as a yellow powder: mp 203−204 °C; ^{1}H NMR ($CDCl_3$) δ = 7.19 (s, 2H, ArH), 6.61 (s, 2H, ArH), 4.28 (t, 8H, J = 7.5 Hz, OCH_2), 3.21−3.08 (2 × t, 16H, SCH_2), 2.71 (t, 8H, J = 6.7 Hz, CH_2CN), 1.35 (s, 36H, $C(CH_3)_3$); ^{13}C NMR ($CDCl_3$) δ = 155.54, 131.20, 128.96, 126.80, 125.41, 117.56, 101.80, 67.38, 34.50, 33.99, 31.30, 30.82, 30.19, 18.92; MS (FAB) m/z = 1426 (M^+). Anal. Calcd for $C_{60}H_{72}N_4O_4S_{16}$·0.5CH_2Cl_2 (1468.68): C, 49.48; H, 5.01; N, 3.81. Found: C, 49.51; H, 4.94; N, 3.83.

(15) Alternative procedures for preparing TTF-*belts*: (a) Adam, M.; Enkelmann, V.; Räder, H.-J.; Röhrich, J.; Müllen, K. *Angew. Chem., Int. Ed. Engl.* **1992**, *31*, 309. (b) Matsuo, K.; Takimiya, K.; Aso, Y.; Otsubo, T.; Ogura, F. *Chem. Lett.* **1995**, 523.

(16) Compound **10a**: Route i: To a solution of **9a** (0.119 g, 0.0837 mmol) in dry DMF (30 mL) was added 0.5 M NaOMe/MeOH (0.75 mL, 0.375 mmol), under N_2. After stirring for 30 min, this mixture and a solution of **2a** (0.0731 g, 0.168 mmol) in dry DMF (30 mL) were simultaneously added over 4 h to dry DMF (30 mL). Then the solvent was removed in vacuo and the residue subjected to column chromatography [silica, CH_2Cl_2/cyclohexane 1:3]. Recrystallization from $CHCl_3$/MeOH afforded **10a** (0.101 g, 68%) as a yellow powder: mp >200 °C dec; ^{1}H NMR ($CDCl_3$) δ = 7.17 (s, 4H, ArH), 6.68 (s, 4H, ArH), 4.32 (t, 16H, J = 8.6 Hz, OCH_2), 3.20 (m, 8H, SCH_2), 3.10 (m, 8H, SCH_2), 1.32 (s, 72H, $C(CH_3)_3$); ^{13}C NMR ($CDCl_3$) δ = 155.56, 131.49, 127.15, 125.46, 118.73, 102.46, 68.00, 34.52, 33.81, 30.20; MS(FAB) m/z = 1762 (M^+). Anal. Calcd for $C_{84}H_{112}O_8S_{16}$ (1762.76): C, 57.24; H, 6.40; S, 29.10. Found: C, 57.02; H, 6.31; S, 28.81. Route ii: To a solution of **11** (0.131 g, 0.240 mmol) in dry DMF (50 mL) was added a solution of CsOH·H_2O (0.088 g, 0.524 mmol) in dry MeOH (5 mL) over 20 min, under N_2. After stirring for 30 min, this mixture and a solution of **2a** (0.105 g, 0.241 mmol) in dry DMF (47 mL) were simultaneously added over 15 h to dry DMF (30 mL). The mixture was stirred for a couple of hours, after which a few drops of a 0.1 M CF_3-COOH/DMF solution were added, which resulted in a color change from red-orange to red-brown. Then CsOH·H_2O (0.088 g, 0.524 mmol) in dry MeOH (5 mL) was added. After stirring for 20 min, this mixture and a solution of **2a** (0.107 g, 0.245 mmol) in dry DMF were simultaneously added over 4 h to dry DMF (30 mL). After stirring for 30 min, the mixture was concentrated in vacuo. Column chromatography [silica, (i) CH_2Cl_2/petroleum ether 1:1; (ii) CH_2Cl_2/petroleum ether 3:1] followed by recrystallization from $CHCl_3$/MeOH afforded **10a** (0.095 g, 45%) as a yellow powder. Route iii: To a solution of **11** (0.121 g, 0.222 mmol) in dry DMF (40 mL) was added CsOH·H_2O (0.169 g, 1.01 mmol) in dry MeOH (6 mL), under N_2. After stirring for 30 min, this mixture and a solution of **2a** (0.197 g, 0.452 mmol) in dry DMF (50 mL) were simultaneously added over 17 h to dry DMF (30 mL). The mixture was stirred for a couple of hours and then concentrated in vacuo. The residue was subjected to column chromatography [silica, (i) CH_2Cl_2/cyclohexane 1: 4; (ii) CH_2Cl_2/cyclohexane 1:2]. The first orange fraction was recrystallized from $CHCl_3$/MeOH to yield **10a** (0.0685 g, 35%) as a yellow powder. The second orange fraction was recrystallized from $CHCl_3$/MeOH to yield **12a** (0.009 g, 5%) as a yellow powder. **12a**: mp >200 °C; ^{1}H NMR ($CDCl_3$) δ = 7.13 (s, 4H, ArH), 7.05 (s, 4H, ArH), 4.31 (t, 16H, J = 4.1 Hz, OCH_2), 3.26 (t, 16H, J = 1.9 Hz, SCH_2), 1.30 (s, 72H, $C(CH_3)_3$); MS(FAB) m/z =1762 (M^+).

(17) (a) Li, Z.-T.; Stein, P. C.; Svenstrup, N.; Lund, K. H.; Becher, J. *Angew. Chem., Int. Ed. Engl.* **1995**, *34*, 2524. (b) Li, Z.-T.; Stein, P. C.; Becher, J.; Jensen, D.; Mørk, P.; Svenstrup, N. *Chem. Eur. J.* **1996**, *2*, 624. (c) Li, Z.-T.; Becher, J. *Chem. Commun.* **1996**, 639. (d) Nielsen, M. B.; Li, Z.-T.; Becher, J. *J. Mater. Chem.* **1997**, *7*, 1175.

(18) For studies on acid-catalyzed isomerization of TTF, see: Souizi, A.; Robert, A. *J. Org. Chem.* **1987**, *52*, 1610.

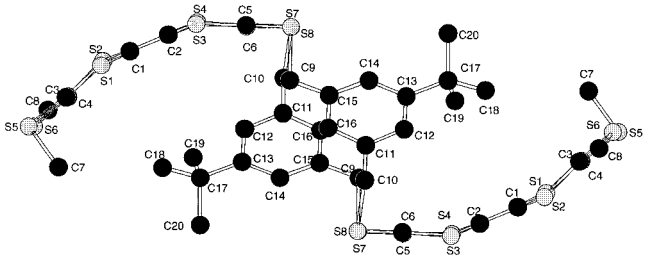

Figure 1. X-ray crystal structure of **4b**.

Scheme 7. Formation of Belts vs Bis-Crowns, the Linker Size Determining the Course of the Reaction

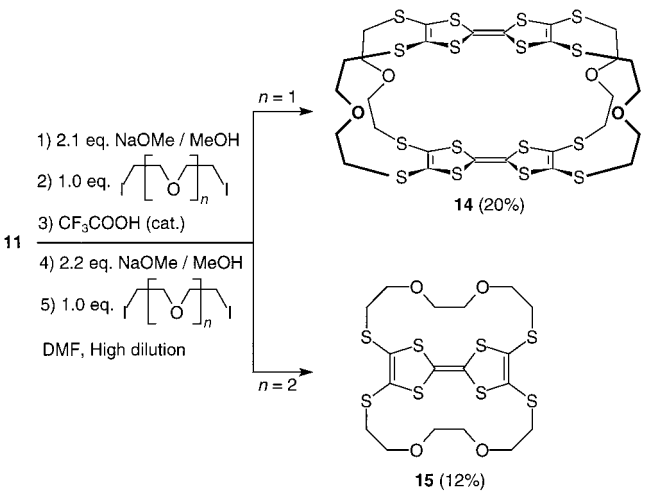

Using the stepwise strategy (route ii) we were able to obtain the bis(ethylene)glycol bridged TTF-belt **14** in a yield of 20% (Scheme 7). However, when extending the length and flexibility of the bridge by using 1,2-bis(2-iodoethoxy)ethane as the alkylating reagent, only the TTF-biscrown **15** was obtained, and no TTF-belt was isolated.

X-ray Crystallography and Semiempirical Calculations. X-ray analysis[19] of **4b** showed that the two TTF units adopted an *S*-type conformation in the solid-state, preventing intramolecular interactions between the TTFs (Figure 1). In this conformation, the steric interactions between the two bulky *tert*-butyl substituents seem to be minimized. As shown in Figure 2, the molecules adopt close intermolecular S−S contacts shorter than the sum of the van der Waals radii (3.7 Å) along the three directions of space. Each molecule has 12 S−S contacts, varying between 3.431(5) and 3.585(7) Å, with adjacent molecules.

Semiempirical PM3 geometry optimizations of **4b** were carried out from different starting geometries employing the Gaussian 98 program package.[20] The first optimization was started from a *U*-type conformation with an interplanar distance of about 5 Å (Figure 3). Optimization disrupts this *U*-form by forcing the two TTFs away from each other into a more

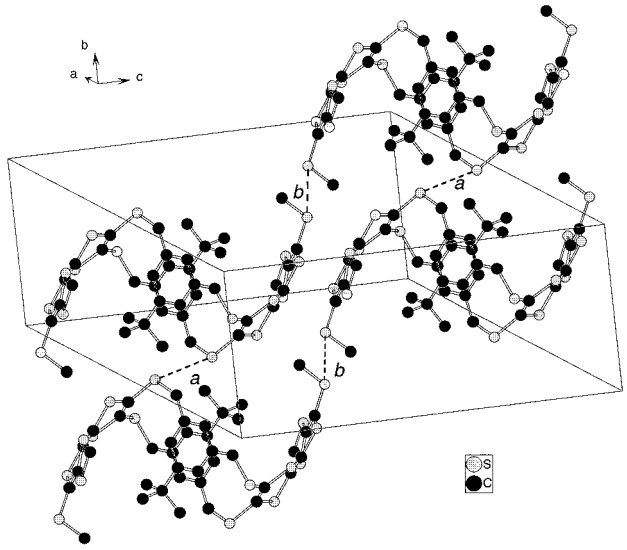

Figure 2. Stereodrawing of the packing diagram of **4b** showing some of the intermolecular contacts: a = distance(S8−S8) = 3.431(5) Å, b = distance(S5−S5) = 3.585(7) Å.

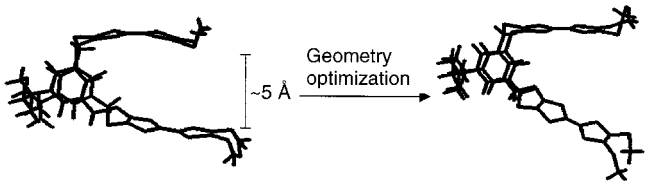

Figure 3. PM3 geometry optimization of **4b,** starting from a *U*-conformation.

V-shaped conformation. From other starting geometries, we obtained *S*- and *V*-shaped structures that possess about the same energy (±7 kcal mol^{-1}), taking into account the large number of atoms. Thus, none of these conformations allows intramolecular $\pi-\pi$ interactions between the two TTFs.

Cyclic Voltammetry. The electrochemical behavior of the bis-TTFs showed that the voltammograms, composed of two oxidation waves, depended on the length and flexibility of the bridge. Indeed, a broadening or a splitting of the first oxidation wave was observed when the flexibility of the bridge decreased. Thin-layer cyclic voltammetry (TLCV)[21] revealed that this first oxidation involves either a one-step two-electron process or two one-electron processes per one unit of bis-TTF. The second oxidation and final step is a two-electron process leading to two fully oxidized TTFs. The TLCV of **4b** revealed two one-electron processes and one two-electron process. The splitting of the first wave may be accounted for by either of the above models (1 or 2). In the case of a model 1 mechanism, the electron ratio obtained by TLCV corresponded to processes involving two, two, and four electrons, respectively, per two units of **4b**. In the next section, we will show that this mechanism is the operating one for the oxidation of **4b** and that it originates from the rigidity of the linkers. Cyclic voltammetry data were collected, together with spectroelectrochemical data (vide infra), in Table 1.

Spectroelectrochemistry. First, we investigated the spectroelectrochemistry[22] of tetramethylthiotetrathiafulvalene (TMT-TTF), the monomeric unit of the synthesized bis-TTFs. One-electron oxidation of TMT-TTF in dichloromethane led to the appearance of an absorption band with a maximum around 470

(19) Single crystals of **4b** were obtained after recrystallisation from CH_2Cl_2/EtOH with a few drops of C_6H_5Cl at 276 K. A yellow single crystal of **4b** was selected by optical examination. X-ray data were collected at 294 K on an Enraf Nonius Mach 3 four circles diffractometer equipped with a graphite monochromator utilizing Mo Kα radiation (λ = 0.71073 Å). The structure was solved by direct methods (SIR) using MolEN package programs [Crystal Structure Analysis: Molecular Enraf-Nonius (MolEN), 1990, Delft Instruments X-ray Diffraction, B. V. Rontnenweg 1, 2624 BD Delft, The Netherlands] and was refined on *F* by the full-matrix least-squares method using anisotropic thermal parameters for S and isotropic ones for C. No absorption corrections were made. The H atoms were included in the calculation without refinement.

(20) M. J. Frisch et al. Gaussian 98, Revision A.7; Gaussian, Inc.: Pittsburgh, PA, 1998.

(21) Thin-layer cyclic voltammetry was performed using a Pt electrode of area 0.0314 cm^2; thin-layer conditions were close to 20 μm. A scan rate of 5 mV s^{-1} was used.

Table 1. Spectroelectrochemical Data in CH_2Cl_2 Containing 0.4 M Bu_4NPF_6

compd	E_1 (V)[a]	E_1' (V)[a]	E_2 (V)[a]	E_{app} (V)[b]	radical cation[c] λ_{max} (nm)	π-dimer λ_{max} (nm)	MV complex λ_{max} (nm)	E_{app} (V)[b]	dication[c] λ_{max} (nm)
TMT-TTF	0.52		0.86	0.67	470	840		0.91	660
3a	0.55		0.87	0.67	460	810		0.91	650
4a	0.54		0.87	0.67	460	790		0.91	650
3b	0.56[d]		0.88	0.67	470	810		0.91	640
4b	0.48	0.64	0.92	0.65	470	820	2300	0.91	650
16	0.47		0.84	0.64	440	770, 1000		0.89	630
14	0.53		1.00	0.66	460	660		1.11	540
10a	0.73		1.16	0.81	470	740[c]		1.17	670

[a] Half-wave potentials (vs Ag/AgCl) obtained by cyclic voltammetry. Concentration of TMT-TTF, 5 mM; all other compounds, 1.25 mM. [b] Applied potential at which the absorption spectrum was measured and the maxima evaluated. [c] Per each unit of TTF. [d] Broad.

nm, which can be assigned to an intramolecular transition of the radical cation, TMT-TTF$^{\bullet+}$.[23] Moreover, formation of the π-dimer (TMT-TTF)$_2^{2+}$ results in an intermolecular charge-transfer absorption band at $\lambda_{max} = 840$ nm. The ratio between the inter- and intramolecular absorptions did not change significantly in the concentration range 0.5−2.5 mM, which means that the equilibrium constant for the dimerization is very high in CH_2Cl_2. From experiments in which the radical cation was generated by chemical oxidation ($NOPF_4$) in CH_2Cl_2, no concentration dependence (measured by UV−vis) was observed between 10^{-7} and 10^{-3} M. The same results were observed in CH_3CN. In this concentration range, the radical cation was soluble, and no precipitation was observed. Under these conditions, the equilibrium constant can be estimated to be $\geq 10^9$ M^{-1}, which corresponds to a ratio of [(TMT-TTF)$_2^{2+}$]/[TMT-TTF$^{\bullet+}$] that is close to 10 at 10^{-7} M. Consequently, the dimerization kinetic constant must be higher than 10^9 $s^{-1}M^{-1}$ in order to be coherent with the electrochemical data, that is, two reversible oxidation processes. Indeed, it was not possible to observe an ESR signal in an ESR spectroelectrochemical experiment,[24] because of the very small concentration of unassociated radical cations.[25] This observation, together with earlier studies,[4] makes the interpretation of the band at 840 nm as an intermolecular interaction in a dimer complex reliable. Moreover, the intrinsic radical cation absorption band at 470 nm must originate mainly from dimerized radical cations. The fact that no precipitation was observed in the chemical oxidation experiment makes it unlikely to occur during the spectroelectrochemical experiment. Moreover, any precipitation should result in an adsorption phenomenum (shape of the wave) in the cyclic voltammogram, which was not the case. Our choice of using CH_2Cl_2 as solvent was, first of all, based on the solubility of the bis-TTFs, because these were not soluble in CH_3CN. Because the CVs of the bis-TTFs did not show any adsorption phenomena either, we can exclude that precipitation of their radical cations occurs within the concentration range of the experiments.

Further oxidation generates the dication TMT-TTF^{2+}, which shows an absorption band around $\lambda_{max} = 660$ nm as the only remaining spectral feature.[26] The emergence of the band in the oxidation progress, after the disappearance of the intra- and intermolecular radical cation absorptions, makes us very confident about its assignment, even though it is shifted significantly from the value reported for the dication transition of TTF^{2+} in acetonitrile ($\lambda_{max} = 390$ nm).[4] Delocalization of the positive charges in TMT-TTF^{2+} onto the SMe groups is a possible and reasonable explanation for this difference.

The spectroelectrochemical data for **3a** and **4a** appeared very similar (Table 1). For both compounds, the ratio between the intrinsic radical cation (referring to one TTF monomer unit) absorption and the π-dimer absorption was almost unaltered upon dilution (concentration range, 0.3−1.4 mM). This concentration independence suggests that the π-dimers,to a high extent, are formed intramolecularly according to a model 1 oxidation. For two TTF radical cations to interact, a distance of about 3.5 Å is required.[27] Indeed, the flexibility of the linkers facilitates the formation of such intramolecular complexes, which involve less Coulombic repulsion than do tetracationic intermolecular (**3a**)$_2^{4+}$/(**4a**)$_2^{4+}$ complexes. The fact that only one wave for the two-electron oxidation generating the diradicals (**3a**)$^{2+}$ and (**4a**)$^{2+}$ is observed in the voltammograms of **3a** and **4a** ($E_1' \leq E_1$) reflects that the formation of π-dimers is favored relative to the formation of MV complexes. The ability of bis-TTFs containing flexible linkers to form intramolecular π-dimers was earlier observed in the crystal structures of divalent cation salts of 2,3-cyclized bis-TTF macrocycles containing S(CH_2-$CH_2O)_nCH_2CH_2S$ ($n = 1$, 2) bridges.[28] Moreover, spectroelectrochemical experiments in solution have revealed intramolecular aggregation of TTF radical cations in a (TTF)$_{21}$-glycol dendrimer in which flexible polyether spacers allow TTFs in close spatial contact to interact.[29]

(22) Spectroelectrochemical experiments were performed in a cell made of Teflon. A 2-mm-diameter stationary platinum disk, polished to a mirror finish, was used as the working electrode. As the counter electrode, a platinum wire was employed. All experiments were performed at an optical path length close to 200 μm. A Lambda 19 Perkin-Elmer spectrophotometer was employed. The current was provided by an EGG PAR 273 potentiostat; a scan rate of 1.25 mV s^{-1} was used. HPLC-grade dichloromethane was used as the solvent and *n*-Bu_4NPF_6 (0.4 M) was used as the supporting electrolyte in all of the experiments. For more details, see: Gaillard, F.; Levillain, E. *J. Electroanal. Chem.* **1995**, *398*, 77.

(23) Earlier studies of the TMT-TTF radical cation in acetonitrile have revealed the following absorption maxima: (i) 461, 366, 329, and 262 nm. Moses, P. R.; Chambers, J. Q. *J. Am. Chem. Soc.* **1974**, *96*, 945. (ii) 850, 560 (sh), 480 (sh), 454, and 261 nm. Kreicberga, J.; Neilands, O. *Zh. Org. Khim.* **1985**, *21*, 2009. We were able to reproduce about the same values as reported by Kreicberga and Neilands in acetonitrile by chemical oxidation ($NOPF_4$) of TMT-TTF at room temperature. In our opinion, these absorptions should be assigned to either intermolecular or intramolecular absorptions within the π-dimer. See main text for discussion. The dimerization of TMT-TTF radical cations is strong in both CH_2Cl_2 and CH_3CN. This enhanced ability of TMT-TTF relative to TTF to form dimers is probably a result of the four extra sulfur atoms which can facilitate dimer formation by favorable S−S interactions.

(24) ESR experiments were run on a Bruker ESP 300 spectrometer driven by the Bruker ESP 1600 computer program. Using this same equipment, similar experiments probing dimer formation of tetrathienylenevinylenes were carried out earlier: Levillain, E.; Roncali, J. *J. Am. Chem. Soc.* **1999**, *121*, 8760.

(25) In contradiction to this experiment, Moses and Chambers[23] measured an ESR signal in their studies of the TMT-TTF radical cation. However, in light of their deviating spectral data, we question if their solution did, in fact, contain the pure and fully mono-oxidized TMT-TTF.

(26) For the TMT-TTF dication Moses and Chambers[23] report the following absorption maxima in acetonitrile: 710, 488, and 456 nm. By chemical oxidation ($NOPF_4$) of TMT-TTF in acetonitrile we obtained almost the same low-energy absorption ($\lambda_{max} = 706$ nm), which is in good agreement with the spectroelectrochemical result, whereas neither of our experiments substantiate the two high-energy absorptions.

(27) Phillips, T. E.; Kistenmacher, T. J.; Ferraris, J. P.; Cowan, D. O. *J. Chem. Soc., Chem. Commun.* **1973**, 471.

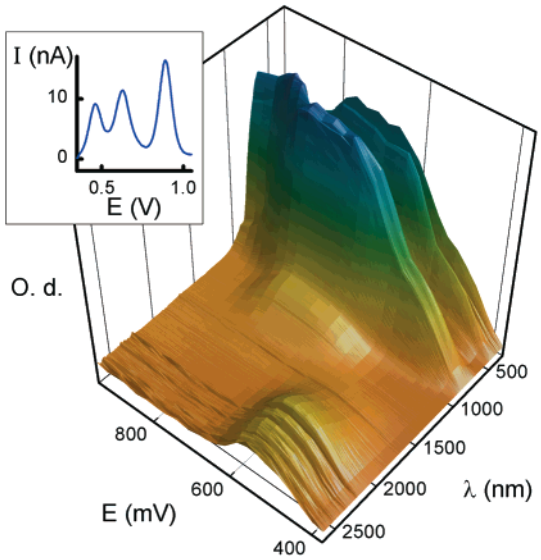

Figure 4. Spectroelectrochemical data for **4b** (1 mM in CH_2Cl_2 containing 0.4 M Bu_4NPF_6).

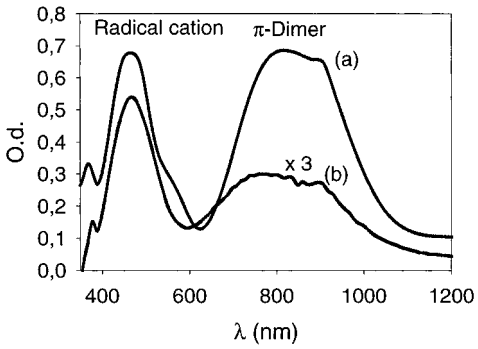

Figure 5. Absorption spectra (at 0.65 V) of **4b** at (a) 1.25 mV and (b) 0.25 mM, in CH_2Cl_2 containing 0.4 M Bu_4NPF_6. Note that the spectrum in (b) has been multiplied by a factor of 3. (Radical cation refers to one unit of TTF.)

The monobridged compound **3b** showed a broadening of the first oxidation wave in the voltammogram. For the related macrocycle **4b,** a significant splitting of the first wave was observed, which can be explained by a strong propensity to form MV complexes. An absorption band at $\lambda_{max} = 2300$ nm (Figure 4), unambiguously assigned to the MV state, developed during the first oxidation wave and disappeared when the oxidation proceeded. It is noteworthy that this band is the first spectral evidence in solution for this state. A gradual increase of the π-dimer absorption was observed during the oxidation, as finally the MV complex was also converted to the π-dimer. When the sample (1.25 mM) was diluted five times, the absorption band arising from the π-dimers was almost halved relative to the intrinsic radical cation (referring to one TTF monomer unit) absorption (Figure 5). This concentration dependence implies the presence of intermolecular π-dimers $(\mathbf{4b})_2^{4+}$, which are formed in favor of intramolecular π-dimers because of the rigidity of the linkers. It also confirms that this band was assigned correctly in the above discussion. The intrinsic radical cation absorption is now originating from radical cation units not only assembled in π-dimers, that is, from $(\mathbf{4b})_2^{4+}$, $(\mathbf{4b})_2^{2+}$, and possibly $\mathbf{4b}^{2+}$ (being in fast exchange with each another on the time scale of the experiment). In other words, an interplanar distance between two TTF units of about 3.5 Å is difficult to achieve intramolecularly, in accordance with the X-ray crystal structure and semiempirical calculations on the neutral molecule (vide supra). However, whether the intermolecular π-dimers are formed in solution between *V*- or *S*-shaped conformations is difficult to rationalize from the solid- and gas-phase studies of neutral **4b**. Since an intermolecular π-dimer, $(\mathbf{4b})_2^{4+}$, involves a total of 4 positive charges, it is suddenly less favorable than the formation of intermolecular MV complexes. Hence, $K_{MV} > K_{\pi-dim}$, implying $E_1' > E_1$ (eq 3), and two waves are seen in the voltammogram. The difference $E_1' - E_1$ is ca. 0.16 V, resulting in a ratio of $K_{MV}/K_{\pi-dim}$ of ca. 500.

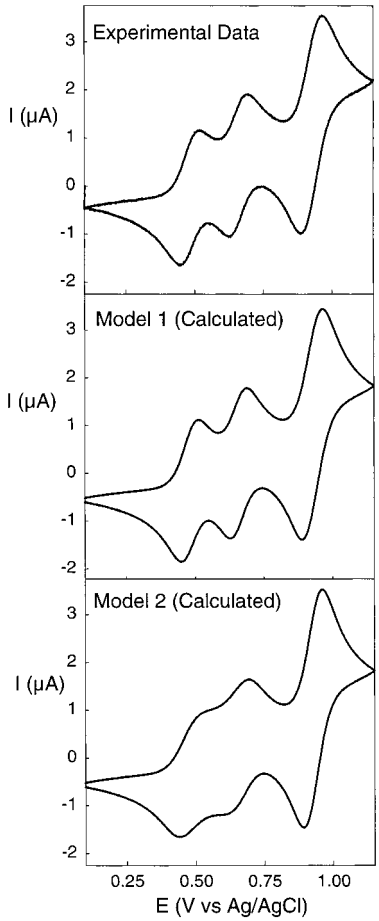

Figure 6. Experimental cyclic voltammogram of **4b** and calculated voltammograms using models 1 and 2 at 0.1 V s^{-1}. For the adjustment, the voltammograms obtained for the experimental scan rates (5, 2, 1, 0.5, 0.2, and 0.1 V s^{-1}) at room temperature are simultaneously taken into account. The reaction rates, k_f, $k_{\pi-dim}$, and k_f, k_{MV}, and the intermolecular π-dimer equilibria have been taken to be arbitrary constants and equal to 10^9 M^{-1} s^{-1} and 0.1 M^{-1}, respectively. The diffusion coefficient, *D*, was 6.7×10^{-6} cm^2 s^{-1}.

From these experiments, we concluded that the MV state occurs intermolecularly and, consequently, model 2, taking into account an intramolecular MV, can be excluded. To raise further support for the model 1 mechanism for the oxidation of **4b**, we carried out theoretical simulations (simulation and fit) of the electrochemical behavior of **4b** (Figure 6). Comparison to the experiment shows qualitatively good agreement.

Spectra of **3b** at high wavelengths did not reveal the absorption band that results from the MV complex, but to judge

(28) (a) Akutagawa, T.; Abe, Y.; Nezu, Y.; Nakamura, T.; Kataoka, M.; Yamanaka, A.; Inoue, K.; Inabe, T.; Christensen, C. A.; Becher, J. *Inorganic Chem.* **1998**, *37*, 2330. (b) Akutagawa, T.; Abe, Y.; Hasegawa, T.; Nakamura, T.; Inabe, T.; Christensen, C. A.; Becher, J. *Chem. Lett.* **2000**, 132.

(29) Christensen, C. A.; Goldenberg, L. M.; Bryce, M. R.; Becher, J. *Chem. Commun.* **1998**, 509.

Table 2. Differential Pulse Data (vs Ag/AgCl) in CH_2Cl_2 Containing 0.1 M Bu_4NPF_6

compd	E_1 (V)	E_1' (V)	E_2 (V)
3b	0.55	0.63	0.91
4b	0.44	0.63	0.90
5	0.46	0.60	0.88
6	0.55	0.63	0.91

from the small separation between E_1 and E_1' in the voltammogram (broad wave), its concentration is much smaller than that of the MV complex of **4b**. However, employing differential pulse voltammetry,[30] it was possible to resolve the first oxidation into two sharp peaks (Table 2). Additionally, compounds **5** and **6** showed a splitting of the first redox potential as a result of MV formation. The splitting is more evident for **5** than for **6**, which can be explained by the difference in the length and, hence, the flexibility of the polyether bridge. Thus, the potentials of **3b** and **6** are almost identical, which means that the extra bridge present in **6** is too flexible to make any difference. In contrast, macrocycle **5** obtains the same large splitting between E_1 and E_1' as macrocycle **4b**.

For comparison, the 2,7(6)-bridged macrocycle **16** was investigated.[17d] The arrangement of the two TTFs in this macrocycle resulted in two very intense absorption bands at maxima of about 770 and 1000 nm upon two-electron oxidation that forms $\mathbf{16}^{2+}$. The intensities of these bands do not decrease relative to the radical cation (referring to one TTF monomer unit) absorption at $\lambda_{max} = 440$ nm upon dilution (1.25−0.25 mM). Thus, the two TTFs are in an ideal arrangement for interacting intramolecularly. The high-energy absorption ($\lambda_{max} = 770$ nm) may be assigned to an intramolecular transition of the diradical, whereas the low-energy absorption ($\lambda_{max} = 1000$ nm) may arise from intramolecular π-dimers, the formation of which is made possible by the flexible polyether linkers, in accordance with the above discussion.

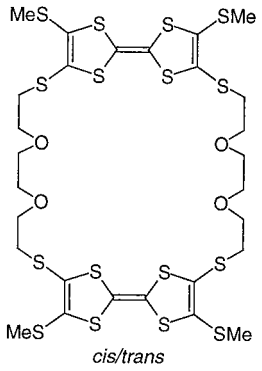

16

The spectrum of the TTF-belt **14** shows an intense, almost concentration-independent absorption band (relative to the intrinsic radical cation absorption in the concentration range 0.25−2.5 mM) at a low wavelength of $\lambda_{max} = 660$ nm which may be assigned to either an intramolecular transition of the diradical or to an intramolecular π-dimer. The face-to-face arrangement of the two TTFs results in a high-energy absorption of the tetracation $\mathbf{14}^{4+}$ at $\lambda_{max} = 540$ nm. Thus, proceeding from TMT-TTF (660 nm) to a dibridged bis-TTF (630−650 nm) and, finally, to a more rigid quadruple-bridged bis-TTF (540 nm)

(30) Differential pulse voltammetry was performed using an Autolab, PGSTAT10 potentiostat (ECO Chemie BV) with *n*-Bu_4NPF_6 as the supporting electrolyte. Counter and working electrodes were made of Pt, and the reference electrode was Ag/AgCl.

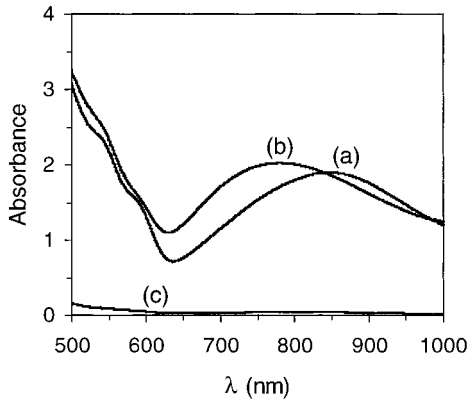

Figure 7. Absorption spectra in CH_2Cl_2 of mixtures of DDQ (3.1×10^{-4} M) with (a) TMT-TTF (6.2×10^{-4} M), (b) **4a** (3.1×10^{-4} M), and (c) **10a** (3.1×10^{-4} M).

results in a gradual increase in the energy of this transition. For the related compound **10a**, a very broad π-dimer absorption band is observed at $\lambda_{max} = 740$ nm. No splitting of the first wave in the voltammograms of **10a** and **14** occurs, signaling that MV complexes are not formed to any significant extent, either intra- or intermolecularly. Moreover, the confinement of two TTFs in a quadruple-bridged arrangement increases the redox potentials of **10a** relative to those of **4a**, that is, electrostatic repulsion between the two TTF mono- or dications is not so easily opposed by conformational changes. For comparison, a strong propensity to form an intramolecular MV state was earlier observed for a criss-cross, overlapped, quadruple-bridged bis-TTF.[31a] A splitting of the second redox potential for criss-crossed, overlapped bis-TTFs was shown to depend highly on the actual linker size.[31]

Complexation Studies. Taking advantage of the electron donating abilities of TTF, we carried out preliminary complexation experiments with different acceptors. However, the strong acceptors 7,7,8,8-tetracyanoethylene-*p*-quinodimethane (TCNQ) and tetracyanoethylene (TCNE) were found to show no significant complexation ability with either **3a** or **4a,** according to ^{1}H NMR experiments in $CDCl_3$. In contrast, 2,3-dichloro-5,6-dicyano-*p*-benzoquinone (DDQ) forms a charge-transfer (CT) complex with **4a** with an absorption at $\lambda_{max} = 780$ nm in CH_2Cl_2 (Figure 7). For the complex of TMT-TTF with DDQ, the CT absorption band appeared at a significantly higher wavelength of $\lambda_{max} = 850$ nm. The difference in absorption maximum may result from the formation of a 1:1 inclusion complex between **4a** and DDQ in which the two TTFs encapsulate one unit of DDQ. A similar inclusion complex between DDQ and a dimeric bisethylenedithiotetrathiafulvalene (BEDT-TTF) was earlier reported by Sugawara and co-workers.[32] To our surprise, the TTF-belt **10a** showed no complexation at all, that is, no complexes are formed in which DDQ is associated either at the outside (alongside) of **10a** or in its cavity. If such outside interactions are neglected for the complexes between **4a** and DDQ, an association constant for the anticipated 1:1 inclusion complex of $K_a = 160$ M^{-1} ($CDCl_3$, 303K) is obtained from ^{1}H NMR dilution experiments employing the chemical shift change of the aryl proton pointing into the cavity. Further work is in

(31) (a) Nielsen, M. B.; Thorup, N.; Becher, J. *J. Chem. Soc., Perkin Trans. 1* **1998**, 1305. (b) Tanabe, J.; Kudo, T.; Okamato, M.; Kawada, Y.; Ono, G.; Izuoka, A.; Sugawara, T. *Chem. Lett.* **1995**, 579. (c) Otsubo, T.; Aso, Y.; Takimiya, K. *Adv. Mater.* **1996**, *8*, 203. (d) Takimiya, K.; Imamura, K.; Shibata, Y.; Aso, Y.; Aso, F.; Ogura, F.; Otsubo, T. *J. Org. Chem.* **1997**, *62*, 5567.

(32) Tachikawa, T.; Izuoka, A.; Sugawara, T. *J. Chem. Soc., Chem. Commun.* **1993**, 1227.

progress to shed more light on the structures of these donor−acceptor complexes.

Conclusions

We have developed simple and high-yielding synthetic procedures for preparing mono-, bis-, and quadruple-bridged dimeric TTFs. The remarkably high yields obtained from any of three synthetic routes of the quadruple-bridged belt molecule **10a** seem to result from preorganization of the reactants. Thus, from simple starting materials, **10a** can be prepared in an overall yield ranging from 30 to 45%. One route takes advantage of the well-known ability of TTF to isomerize in the presence of catalytic amounts of acid. This isomerization reaction is now implemented into the synthetic protocol and can be considered as a standard method to control the isomeric purity in such reactions.

Cyclic voltammetry and spectroelectrochemical measurements clearly demonstrate that both the nature of the linkers and the way in which they are connecting the two TTFs are of importance for controlling the redox potentials and the formation of MV and π-dimers in solution. Upon oxidation of the rigid macrocycle **4b**, MV complexes were generated to such a high extent that we were able to measure its absorption wavelength in solution ($\lambda_{max} = 2300$ nm). The MV absorption of **4b** seems to originate from intermolecular $(\mathbf{4b})_2^{2+}$ complexes, according to measurements at various concentrations and according to cyclic voltammogram simulations. In the presence of more flexible linkers, intramolecular association of radical cations to π-dimers suppresses the formation of MV complexes. These findings are important for both the future design of organic conductors based on TTF as well as supramolecular systems that rely on the different and interconvertible redox states of TTF.[33]

Complexation studies with the electron acceptor DDQ have been carried out. Although the macrocycle **4a** forms a donor−acceptor complex with DDQ, as does TMT-TTF, no complexation is observed for the TTF-belt **10a**, according to UV−vis spectroscopy.

Supporting Information Available: Full experimental procedures; tables of bond distances and angles, positional parameters, and general displacement parameters for **4b**. This material is available free of charge via the Internet at http://pubs.acs.org.

JA000537C

(33) Recent review of TTF in supramolecular chemistry: Nielsen, M. B.; Lomholt, C.; Becher, J. *Chem. Soc. Rev.* **2000**, *29*, 153.